

2021

Thermal Analysis of a Hybrid Air Conditioning System with Geothermal Energy

Shaimaa Mohamed El-hetamy, Alsaid khalil, S. A. El-Agouz, Mohamed Samadony

Follow this and additional works at: <https://digitalcommons.aaru.edu.jo/erjeng>

Recommended Citation

Mohamed El-hetamy, Alsaid khalil, S. A. El-Agouz, Mohamed Samadony, Shaimaa (2021) "Thermal Analysis of a Hybrid Air Conditioning System with Geothermal Energy," *Journal of Engineering Research*: Vol. 5: Iss. 2, Article 1.

Available at: <https://digitalcommons.aaru.edu.jo/erjeng/vol5/iss2/1>

This Article is brought to you for free and open access by Arab Journals Platform. It has been accepted for inclusion in Journal of Engineering Research by an authorized editor. The journal is hosted on [Digital Commons](#), an Elsevier platform. For more information, please contact rakan@aar.edu.jo, marah@aar.edu.jo, u.murad@aar.edu.jo.

Thermal Analysis of a Hybrid Air Conditioning System with Geothermal Energy

A. Khalil^a, S. A. El-Agouz^a, M. O. A. El-Samadony^a and Sh. M. El-Hetamy^b

^aMechanical Power Eng. Department, Faculty of Eng., Tanta Univ., Egypt

^b Higher Institutes for Engineering & Technology, El-Obour, Egypt.

Abstract- Hybrid air conditioning systems can allow significant energy saving and emissions reductions with respect to conventional air-conditioning systems. Thermal analysis of a desiccant wheel, a heat exchanger, a ground source circulation system, and a solar collector for a hybrid air conditioning system is performed in this study. The effects of these parameters have been studied: Inlet air temperature, Inlet air humidity ratio, wheel speed, regeneration temperature, regeneration mass flowrate, heat exchanger effectiveness, ground source circulation effectiveness, and solar radiation on the behavior of the outlet air temperature and the outlet air humidity ratio from the desiccant wheel, the area of solar air collector, the solar collector efficiency, the cooling coil load, and the coefficient of performance. The hybrid system is more efficient than the vapor compression system. The hybrid system significantly decreases the cooling coil load, the cooling coil load of the hybrid system is approximately 48 % lower than the vapor compression system.

Key words- Hybrid air conditional, Ground source circulation, Desiccant wheel, COP_{th}.

1. INTRODUCTION

In conventional cooling systems, humidity of air is removed by condensation. The Coefficient of performance (COP) of the conventional system decreases as the heating after dehumidification is always necessary. Hybrid desiccant dehumidification systems integrated with conventional cooling system can handle latent and sensible loads. Hybrid desiccant cooling systems can also use low grade energy sources or low temperature sources such as solar power, waste heat etc. Solar energy as a heat source for regeneration has also been studied [1,2,3].

Furthermore, [4] found that energy savings ranging from 30% to 50% could be achieved for three different hybrid cycles under Indian climatic conditions. [5] also discovered that energy savings ranging from 30% to 50% could be achieved for three different hybrid cycles under Indian climatic conditions. Thermal comfort for occupants using low grade thermal energy has gained increasing attention, and various types of technologies have been developed [6]. On the basis of mathematical modeling, thermodynamic research, experimental investigation, and practical implementation, rotary desiccant cooling has been widely investigated over a number of years [7].

Several review studies are undertaken by various researchers to describe and operate desiccant cooling systems [8–10]. The most popular desiccant cooling systems, designed by different researchers [11–13], are systems using rotary desiccant wheel to dehumidify air. A thermal analysis of air conditioning system was been studied [14], via its

various components: desiccant wheel, solar collector, heat exchanger, ground heat exchanger, and water spray evaporative cooler. The study simulates three different air conditioning cycles for different zones such as hot-dry, warm-dry, hot-humid, and warm-humid zones, found that the desiccant air conditioning system gives a greater thermal comfort in different climates. They discussed the sensible and latent load of AC needed for nonhuman AC applications [15]. They described ideal temperature and humidity zones, and effective AC systems for the applications were proposed and discussed. Furthermore, the thermodynamic limitations of the VAC method are discussed.

The potential for efficient air-conditioning (AC) and cooling systems to avoid excessive power consumption, as well as the mitigation of harmful refrigerants generated by existing AC systems [16]. Introduced desiccant based air-conditioning (DAC) options for livestock's thermal comfort [17]. Experimentally investigated desiccant dehumidification and indirect evaporative cooling for agricultural product storage, the thermodynamic advantages of the proposed system were highlighted by [18], and it was compared to vapor compression systems. Comprehensive details of evaporative cooling options for building air - conditioning (AC) in Multan (Pakistan) [19].

A solid-silica-gel-based DAC system was developed, at lab-scale, for the performance evaluation of the DAC system [20]. [21] recalled the principle of a solid desiccant cooling system and discussed its technological applications and advancements. Different configurations of desiccant cooling cycles, conventional and hybrid desiccant cooling cycles, various types of mathematical models of rotary desiccant dehumidifier, performance evaluation of desiccant cooling system, technological advancement, and the advantages it can provide in terms of energy and cost savings are highlighted. A detailed account of the general features and performance of the solid desiccant cooling system when powered by solar energy or industrial waste heat for desiccant regeneration are provided.

In this study a mathematical model of the hybrid air conditioning system. The effects of the following parameters are studied: inlet air temperature, inlet air humidity ratio, regeneration air temperature, regeneration mass flowrate, heat exchanger effectiveness, ground source circulation effectiveness, and solar radiation on the behavior of outlet air temperature from desiccant wheel, outlet air humidity ratio from desiccant wheel, area of solar air collector, efficiency of a solar air collector, cooling coil load, and coefficient of performance.

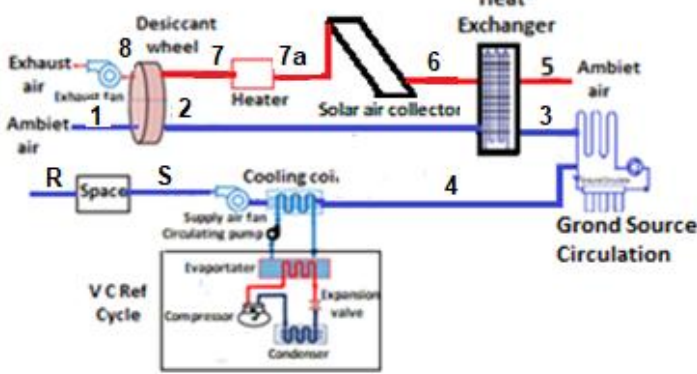


Fig. 1(a)

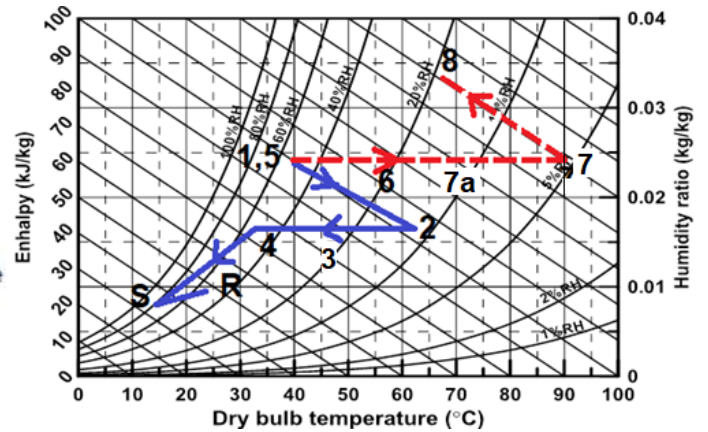


Fig. 1(b)

Fig. 1 Hybrid air conditioning system with desiccant wheel / heat exchanger and ground source circulation. (a) schematic of system, (b) processes of both process air and regeneration air on psychrometric chart.

(1)

1. SYSTEMS DESCRIPTION

The hybrid air conditioning system consists of a desiccant wheel (DW), a heat exchanger (HE), a ground source circulation (GSC), a vapor compression cycle (VCC), a solar air collector (Sol), and auxiliary heater (AH). The desiccant cooling process has two air streams, process (points 1–R) and regeneration (points 5–8), as shown in Fig. 1(a). When the temperature of the solar air collector lower than dehumidification temperature, the auxiliary heater is driven. The ambient air is used to prepare the process air stream and the regeneration air stream. Fig. 1(b) presents the schematic of the process and regeneration air on the psychrometric chart the desiccant wheel is used to dry the process air (1) first. After the process air is dried in the desiccant wheel (2), it is precooled by passing it through the heat exchanger (3), and by passing ground source circulation (4). Thereafter, the precooled air (4) is cooled by passing in cooling coil.

3. GOVERNING EQUATIONS

A. Desiccant wheel

In this section the temperature and humidity of outlet air from the desiccant wheel is calculated using the simulation software of desiccant wheel. A desiccant wheel simulation software was used for the analysis of desiccant cooling cycles, by knowing inlet conditions in points 1 and 7 and also the wheel properties, the simulation of the desiccant wheel can be performed.

B. Heat Exchanger

The purpose of the heat exchanger, is to transfer the heat of absorption that is present in the supply air stream after dehumidification to the regeneration air stream. The effectiveness of an ideal heat exchange system with negligible air leakage and heat transfer to the outdoors is known as

$$\epsilon_{HE} = \frac{T_2 - T_3}{T_2 - T_5}$$

where $T_5 = T_1$ is the ambient temperature. (3) therefore, the exit air temperature at point 3 is

$$T_3 = T_2 - \epsilon_{HE}(T_2 - T_5) \quad (2)$$

The energy balance between the two air streams is written by the following equation:

$$h_6 - h_5 = h_2 - h_3$$

The states at points 3 and 6 are calculated with the above equation and when the temperature and humidity ratio in points 2 and 5 are known, the leakage is negligible, so $\omega_2 = \omega_3$, $\omega_5 = \omega_6 = \omega_1$.

C. Ground Source Circulation

By variations in the air temperature and solar radiation the ground temperature is affected. Under influence of these effects, ground temperature fluctuates daily and annually. The annual variation of the surface ground temperature can be estimated using a sinusoidal function [22]. The ground temperature is changing down to 10 m in depth after which the ground temperature becomes constant [23]. The purpose of the ground source circulation is to cool the supply air stream after the heat exchanger. In the ideal heat exchange system, with negligible air leakage and heat transfer to the outdoors, effectiveness is defined as

$$\epsilon_{GSC} = \frac{T_3 - T_4}{T_3 - T_{w.in}} \quad (4)$$

Therefore, the exit air temperature at point 4 is

$$T_4 = T_3 - \epsilon_{GSC}(T_3 - T_{w.in}) \quad (5)$$

Calculates the enthalpy of moist air at points 3 and 4 where $\omega_3 = \omega_4 = \omega_2$.

D. Solar Air Collector

The energy balance equations in steady state to determine the area of the collector. Energy into a system must be equal to the energy output from the system. To model the collector, a number of assumptions are made which do not contradict

the real situation [24]. The assumptions made are given as follows:

1. The thermal performance of the collector is considered under steady state condition.
2. Temperature of air varies only in the flow direction.
3. The collector components are operating at uniform temperature.
4. Heat lost through the bottom plate is by conduction alone.
5. Compared to the top and bottom the side loss coefficient is negligible.

The first law of thermodynamics along with heat transfer analysis is applied to the various components of the collector and the mathematical expressions are formulated and presented below.

The energy balance in the glass cover is:

$$S_1 + (\tilde{h}_1 + \tilde{h}_{r21})(T_{ap} - T_c) = (\tilde{h}_w + \tilde{h}_{rs})(T_c - T_a) \quad (6)$$

Energy balance on the absorbing plate is:

$$S_2 = (\tilde{h}_1 + \tilde{h}_{r21})(T_a - T_c) + \tilde{h}_{r23}(T_{ap} - T_{bp}) + \tilde{h}_3(T_{ap} - T_f) \quad (7)$$

Energy balance for the fluid:

$$\tilde{h}_3(T_{ap} - T_f) = q_u + \tilde{h}_4(T_f - T_{bp}) \quad (8)$$

Energy balance on the bottom plate

$$\tilde{h}_{r23}(T_{ap} - T_{bp}) + \tilde{h}_4(T_f - T_{bp}) = U_b(T_{bp} - T_a) \quad (9)$$

The difference between the incident solar radiation and the optical loss is used to measure the solar radiation absorbed by the absorbing plate per unit area:

$$S_1 = \alpha I \quad (10)$$

The incident solar radiation that is absorbed by the absorbing plate is represented by

$$S_2 \cong 0.97\tau_c\alpha_{ap}I \quad (11)$$

The heat gain equation is given as:

$$q_u = m_f C_p (T_{fo} - T_{fi}) \quad (12)$$

the collector efficiency can be determined by:

$$\eta_c = \frac{m_f C_p (T_{fo} - T_{fi})}{I} \quad (13)$$

3. CYCLE PERFORMANCE

The thermal Coefficient of Performance (COP_{th}) of the cooling system was determined by the ratio of the cooling load system to the sum of regeneration heat and electrical power input to the vapor compression cycle.

$$COP_{th} = \frac{Q_l}{Q_{Reg} + P_{in}} \quad (14)$$

The regeneration energy gain by the air was determined from:

$$Q_{Reg} = m_{Reg}(h_7 - h_6) \quad (15)$$

P_{in} is the input power for running the vapor compression cycle compressor. The current study does not take into account the energy needed for a circulator pump and

ventilator fan. This assumption separates the results from the distribution system.

4. NUMERICAL PROCEDURES

The above-mentioned governing equations were solved using a computer program. The analysis of desiccant cooling cycles was conducted using desiccant wheel simulation software. The simulation of the desiccant wheel can be done by knowing the inlet conditions in points 1 and 7 as well as the wheel properties. The airstream simulation continues by calculating points 3 and 4 in relation to the equations in "Desiccant Wheel," "Heat Exchanger," "Ground Source Circulation," and "Solar Air Collector." In the regeneration air stream, the outdoor design condition at point 5 is known, and the air regeneration at point 6 can be calculated. Then, using the equations in "Solar Air Collector," the effects of the solar air collector can be calculated.

5. RESULTS AND DISCUSSION

In the present study, the design parameters of the desiccant wheel include wheel speed = (10, 15, 20, 25 and 30 RPH), wheel diameter = 3050 mm and wheel depth = 200 mm. Ground temperature is assumed to be constant at T_{w,in} = 20 °C and ε_{HE} = ε_{GSC} = (0.6, 0.7, 0.8, 0.9) are the effectiveness of heat exchanger, ground source circulation.

A. Effect of the Ambient Air Temperature

Fig. 2 shows the effect of the ambient air temperature, T₁ on of the desiccant wheel's outlet air temperature and outlet air humidity ratio, T₂, w₂. The speed of the desiccant wheel is kept constant at 25 RPH, constant regeneration air temperature at 90 °C, constant ambient air humidity ratio at 24 g_w/kg_{da}, constant heat exchanger effectiveness at 0.9, and Ground source circulation at 0.9. When the inlet air temperature increases, the outlet air temperature and the outlet air humidity ratio of the desiccant wheel in the process air stream increase.

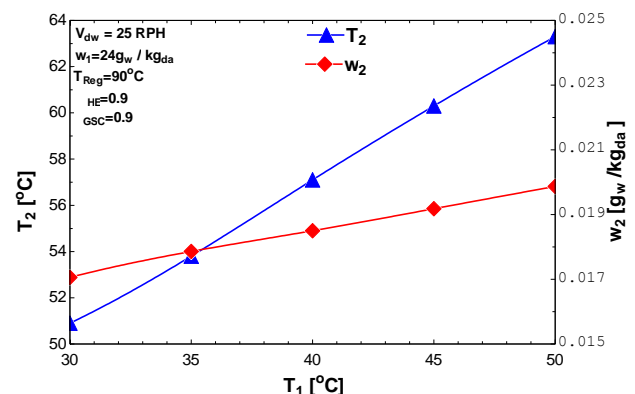


Fig. 2 The effect of inlet air Temperature, on the outlet air conditions from desiccant wheel

Fig. 3 shows the effect of inlet air Temperature, T₁ on the area of sola collector, A_c and solar collector efficiency, η_c at the same parameter on Fig. 3. When the inlet air temperature increases, the area of solar collector decreases and the solar collector efficiency increases. Fig. 4 shows the effect of inlet air Temperature, on cooling coil load and the coefficient of

performance at the same parameter on Fig. 3 and Fig. 4. The cooling coil load of vapor compression cycle increases when the inlet air Temperature increases but the coefficient of performance decreases when the inlet air Temperature.

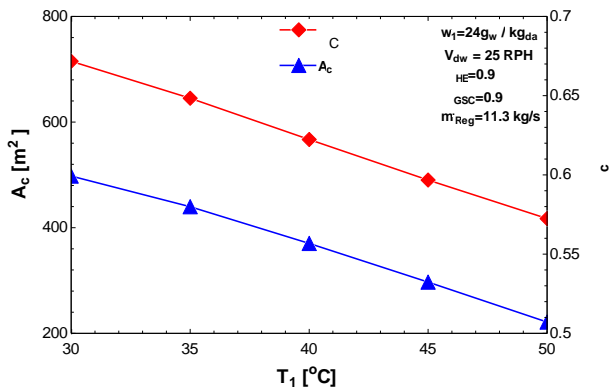


Fig. 3 The effect of inlet air Temperature, on the area of solar collector and the solar collector efficiency.

When outdoor air temperature increases, the outlet air from the desiccant wheel in the process air stream, at point 2, increases. Therefore, the process air stream at the inlet of heat exchanger system at point 3 has the high value, so the outlet air temperature of heat exchanger at the air regeneration process has high value. This is caused that the temperature inlet solar collector is high value, so the area of solar air collector is lower value as shown in Fig. 3, and so the coefficient of performance is lower value as shown in Fig. 4. Increasing inlet air temperature from 30 to 50 °C results in increasing outlet air temperature and outlet air humidity ratio from the desiccant wheel, and cooling coil load by 24, 13, and 33 % respectively, but the area of solar air collector, solar collector efficiency and the coefficient of performance decrease by 55, 14, and 8 % respectively.

B. Effect of the Ambient Air Humidity Ratio

The effect of the ambient air humidity ratio, w_1 on of the desiccant wheel's outlet air temperature and outlet air humidity ratio, T_2 , w_2 is shown in Fig. 5. When the inlet air humidity ratio increases, the outlet air temperature and the outlet air humidity ratio of the desiccant wheel in the process air stream increase, at constant speed of the desiccant wheel at 25 RPH, constant regeneration air temperature at 90 °C, constant ambient air temperature at 40 °C, constant heat exchanger effectiveness at 0.9, and Ground source circulation at 0.9.

At a constant inlet air temperature and for a high humidity ratio, the air leaving the desiccant wheel at the process air stream at point 2, contains more humidity. Therefore, the process air stream at the inlet of heat exchanger system at point 3 has the high temperate and humidity ratio, so the outlet air temperature of heat exchanger at the air regeneration process has lower value.

This is caused that the temperature inlet solar collector is lower value, so the area of solar air collector is high value as shown in Fig. 6, and so the coefficient of performance is lower value as shown in Fig. 7.

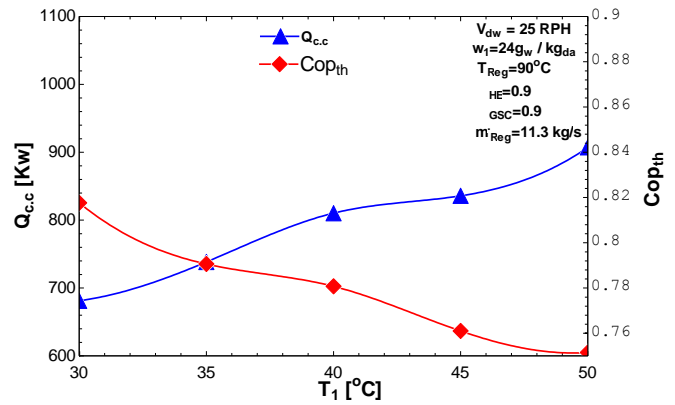


Fig. 4 The effect of inlet air Temperature, on cooling coil load and the coefficient of performance.

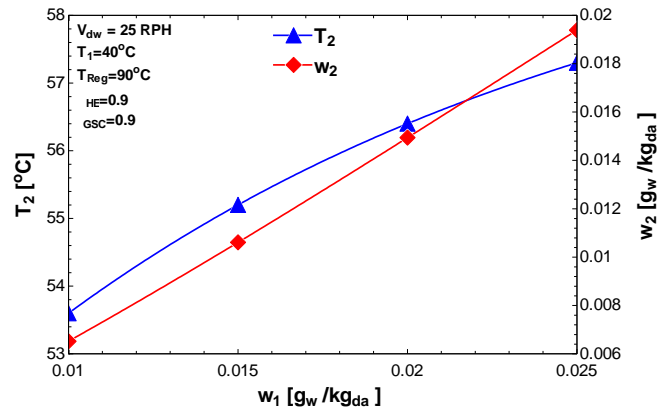


Fig. 5 The effect of inlet air humidity ratio, on the outlet air conditions from desiccant wheel.

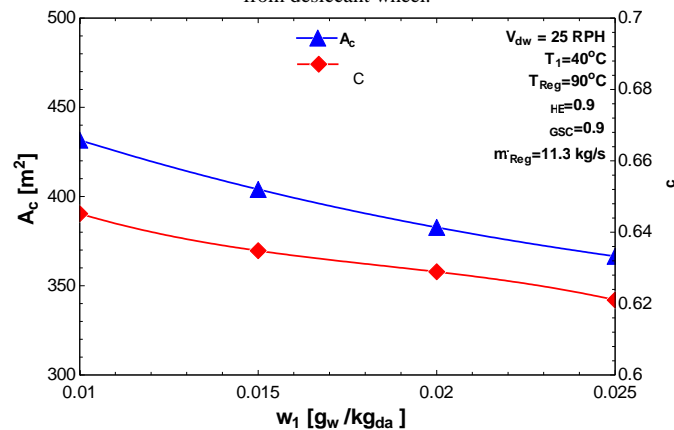


Fig. 6 The effect of inlet air humidity ratio, on the area of solar collector and the solar collector efficiency.

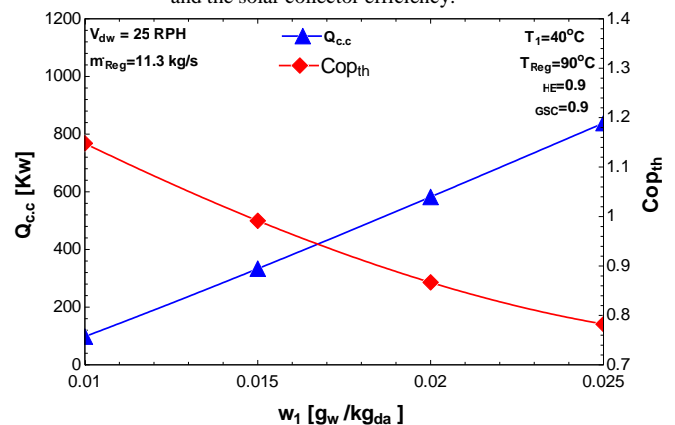


Fig. 7 The effect of inlet air humidity ratio, on cooling coil load and the coefficient of performance.

When humidity ratio increases from 0.01 to 0.025 kg_w/kg_{da} , the outlet air temperature and outlet air humidity ratio from the desiccant wheel, cooling coil load increase by about 7, 197, 700 % respectively, but the area of solar air collector, solar collector efficiency, and the coefficient of performance decrease by 15, 4, and 32% respectively.

C. Effect of the wheel speed

Fig. 8 presents the effect of wheel speed, V on the outlet air conditions from desiccant wheel, T_2 , w_2 . When the wheel speed increases, the outlet air temperature in the process air stream increase, and the outlet air humidity ratio of the desiccant wheel decreases, at constant regeneration air temperature at 90 °C, constant ambient air temperature at 40°C, constant humidity ratio at 24 g_w/kg_{da} constant heat exchanger effectiveness at 0.9, and Ground source circulation at 0.9.

Therefore, the process air stream at the inlet of heat exchanger system at point 3 has the high air temperate and lower air humidity ratio, so the outlet air temperature of heat exchanger at the air regeneration process has high value. This is caused that the temperature inlet solar collector is high value, so the area of solar air collector is lower value as shown in Fig. 9, and so the coefficient of performance is high value as shown in Fig. 10. When wheel speed increases from 10 to 30 RPH, the outlet air temperature from the desiccant wheel, the area of solar air collector, solar collector efficiency, and coefficient of performance increase by about 7, 120, 18, and 5 % respectively, but cooling coil load decreases by the 4 %.

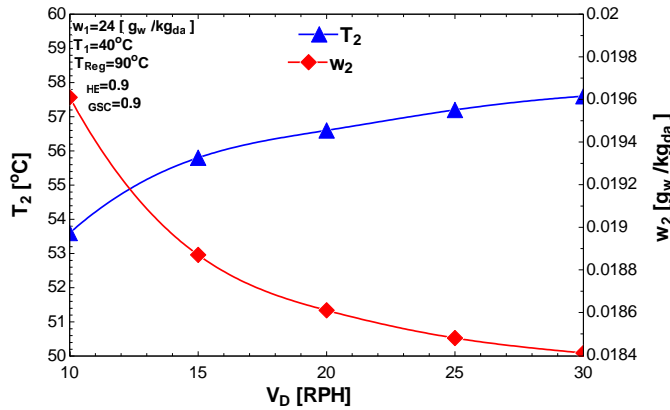


Fig. 8 The effect of wheel speed, on the outlet air conditions from desiccant wheel.

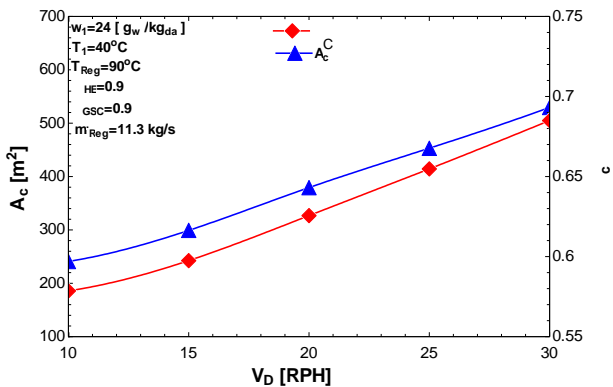


Fig. 9 The effect of wheel speed, on the area of solar collector and the solar collector efficiency.

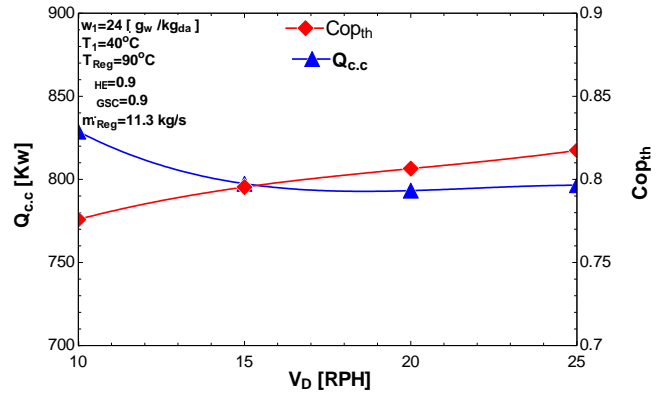


Fig. 10 The effect of wheel speed, on cooling coil load and the coefficient of performance.

D. Effect of the Regeneration Temperature

Fig. 11 presents the effect of the regeneration temperature, T_{Reg} on the outlet air conditions from desiccant wheel, T_2 , w_2 . When the regeneration temperature increases, the outlet air temperature in the process air stream increases, but the outlet air humidity ratio of the desiccant wheel decreases, at constant speed of the desiccant wheel at 25 RPH, constant ambient air temperature at 40°C, constant humidity ratio at 24 g_w/kg_{da} constant heat exchanger effectiveness at 0.9, and Ground source circulation at 0.9.

Therefore, the process air stream at the inlet of heat exchanger system at point 3 has the high air temperate and lower air humidity ratio. So, the outlet air temperature of heat exchanger at the air regeneration process has lower value, this is caused that the temperature inlet solar collector is lower value, so the area of solar air collector is high value as shown in Fig. 12, and so the coefficient of performance is lower value as shown in Fig. 13. When the regeneration temperature increases from 70 to 120 °C, the outlet air temperature from the desiccant wheel, the area of solar air collector, and solar collector efficiency, increase by about 30, 37, 4, and 5 % respectively, but the outlet air humidity ratio from the desiccant wheel, the cooling coil load, and the coefficient of performance decrease by 20, 22 and 80 %.

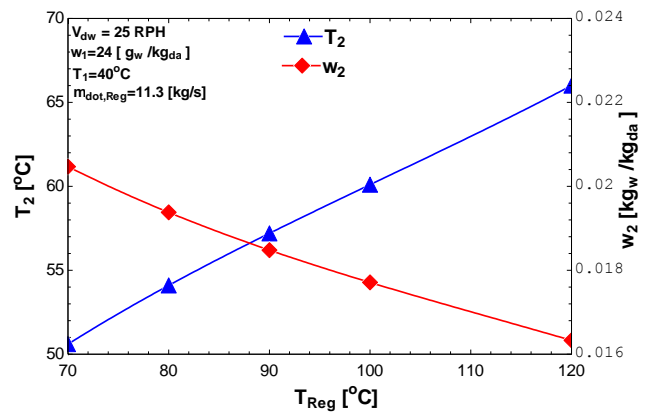


Fig. 11 The effect of regeneration air temperature, on the outlet air conditions from desiccant wheel.

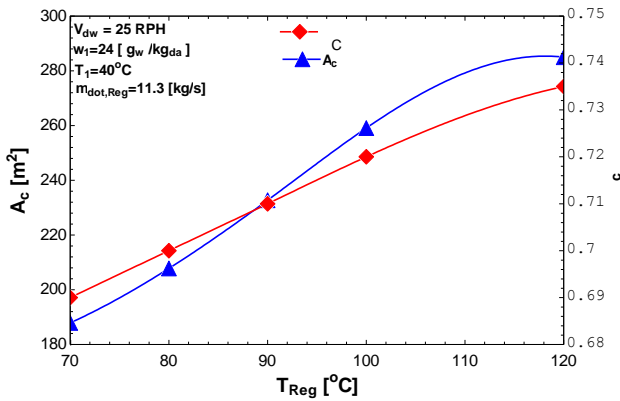


Fig. 12 The effect of regeneration air temperature, on the area of solar collector and the solar collector efficiency

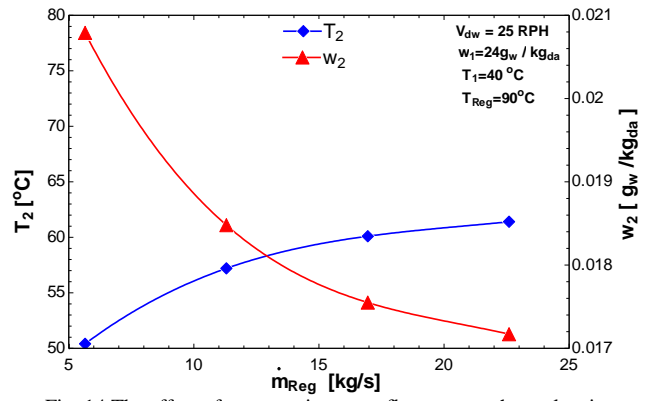


Fig. 14 The effect of regeneration mass flowrate, on the outlet air conditions from desiccant wheel.

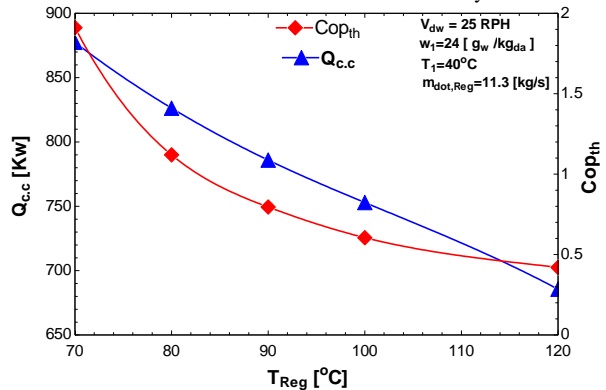


Fig. 13 The effect of regeneration air temperature, on cooling coil load and the coefficient of performance.

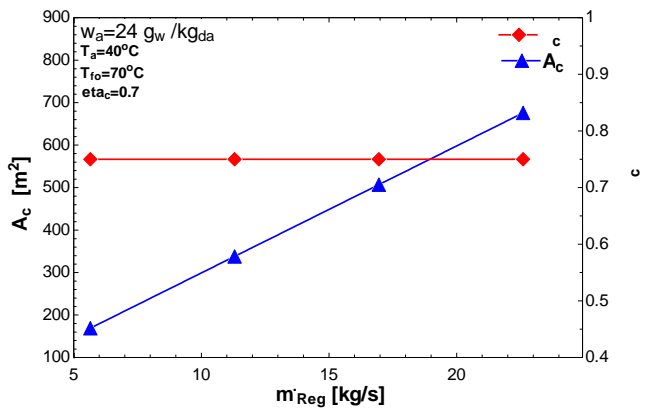


Fig. 15 The effect of regeneration mass flowrate, on the area of solar collector and the solar collector efficiency.

E. Effect of the regeneration mass flowrate

The effect of the regeneration mass flowrate, m_{reg} on the outlet air conditions from desiccant wheel, T_2 , w_2 is shown in Fig. 14. When the regeneration mass flowrate increases, the outlet air temperature in the process air stream increases, but the outlet air humidity ratio of the desiccant wheel decreases, at constant speed of the desiccant wheel at 25 RPH, constant ambient air temperature at 40 °C, constant humidity ratio at 24 g_w/kg_{da} , constant regeneration temperature at 90°C constant heat exchanger effectiveness at 0.9, and Ground source circulation at 0.9.

As the high regeneration mass flowrate, the area of solar air collector is high and solar collector efficiency is constant as shown in Fig. 15, and so the coefficient of performance and the cooling coil load are lower value as shown in Fig. 16. When the regeneration mass flowrate increases from 5.65 to 22.6 kg/s, the outlet air temperature from the desiccant wheel, the area of solar air collector, increase by about 22, and 500 % respectively, but the outlet air humidity ratio from the desiccant wheel, the cooling coil load, and the coefficient of performance decrease by, 17, 22, and 51 %.

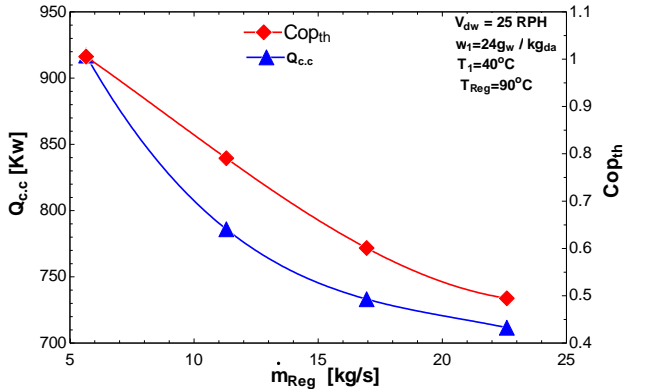


Fig. 16 The effect of regeneration mass flowrate, on cooling coil load and the coefficient of performance.

F. Effect of the heat exchanger effectiveness

Fig. 17 and Fig. 18 present the effect of the heat exchanger effectiveness, ϵ_{HE} on the area of collector, collector efficiency, on cooling coil load and the coefficient of performance. When the heat exchanger effectiveness increases from 0.6 to 0.9, the solar collector efficiency and the coefficient of performance increase by about 9, and 4 % respectively. but the area of collector, and the cooling coil load decrease by about 8, and 2 % respectively.

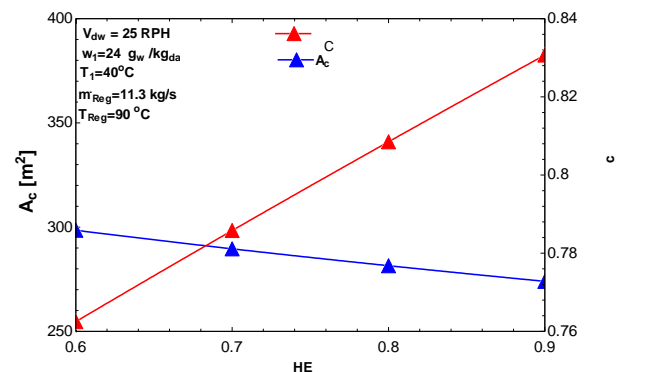


Fig. 17 The effect of heat exchanger effectiveness, on the area of collector and collector efficiency

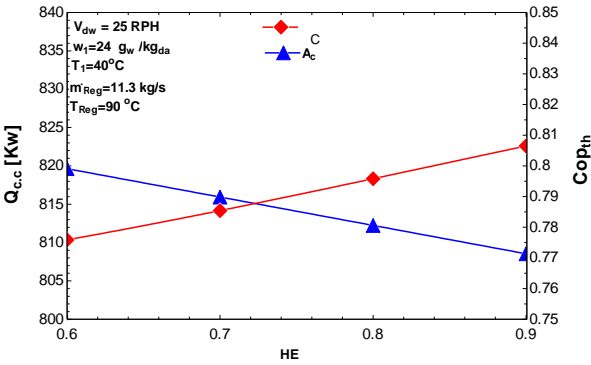


Fig. 18 The effect of heat exchanger effectiveness, on the area of solar collector and the solar collector efficiency.

G. Effect of the ground source circulation effectiveness

The effect of the ground source circulation effectiveness, ϵ_{GSC} on the cooling coil load and the coefficient of performance is presented Fig. 19. When the ground source circulation effectiveness increases, the coefficient of performance increases, while the cooling coil load decreases. When the ground source circulation effectiveness increases from 0.6 to 0.9, the coefficient of performance increases by 11 %, but the cooling coil load decreases by about 15 %.

H. Effect of Solar Radiation

The effect of solar radiation, I on the area of solar collector and the solar collector efficiency are shown in Fig. 20. The area of solar collector decreases, while the solar collector efficiency increases by the solar radiation increases. When the solar radiation increases from 532.6 to 1005 w/m^2 , the solar collector efficiency increases by about 39 %, while the area of solar collector decreases by about 62 %.

I. Comparison between the hybrid system and the vapor compression system

Fig. 21 and Fig. 22 show the variation of the cooling coil load with inlet air temperature and inlet air humidity ratio for a hybrid system and vapor compression system. As shown in figures the cooling coil load in a hybrid system is lower than that the vapor compression system. When inlet air temperature increases from 30 to 50°C, the cooling coil load of the hybrid system is approximately 49 % lower than the vapor compression system. When inlet air humidity ratio increases from 0.01 to 0.024 kg_w/kg_{da} , the cooling coil load of the hybrid system is approximately 47 % lower than the vapor compression system. Therefore, it is clear that the hybrid system is more efficient than the vapor compression system.

7. CONCLUSION

In this study, the hybrid air conditioning system consisting of a desiccant wheel, a heat exchanger, a ground source circulation, a solar air collector, and vapor compression cycle, the heat obtained from a ground source and solar radiation was utilized. The main conclusions from the results of this study, are as follows:

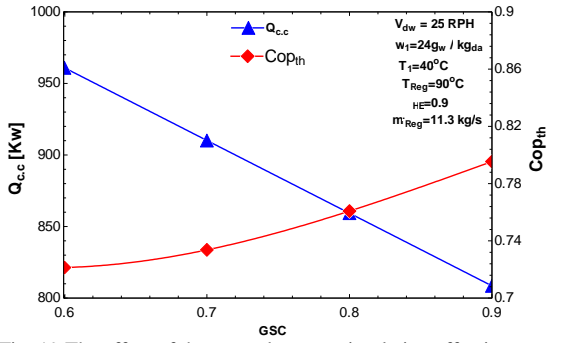


Fig. 19 The effect of the ground source circulation effectiveness, on cooling coil load and the coefficient of performance.

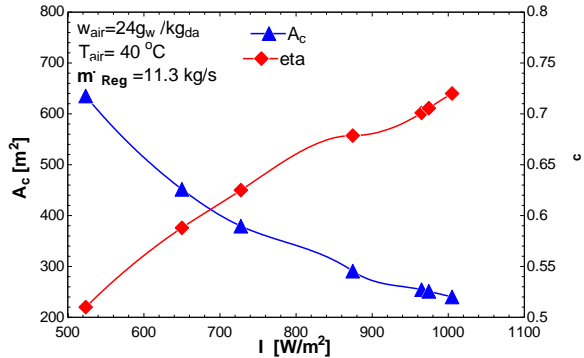


Fig. 20 The effect of solar radiation on the area of solar collector and the solar collector efficiency.

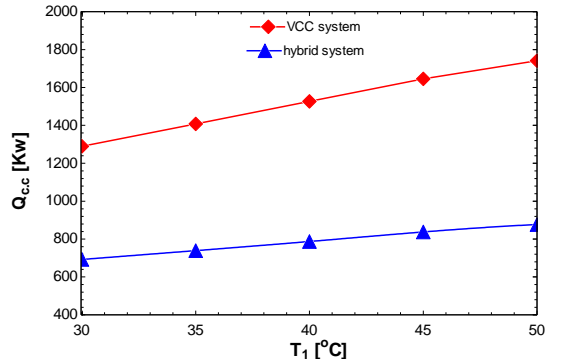


Fig. 21 Variation of cooling coil load with inlet air temperature for a hybrid system and vapor compression system.

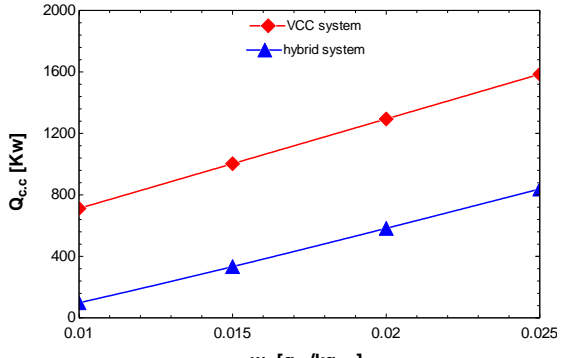


Fig. 22 Variation of cooling coil load with inlet air humidity ratio for a hybrid system and vapor compression system.

1. The outlet air temperature from desiccant wheel T_2 increases with the increase of inlet air temperature, and inlet air humidity ratio, wheel speed, regeneration air temperature, and regeneration mass flowrate.

2. The outlet air humidity ratio from desiccant wheel w_2 increases with the increase of inlet air temperature, and inlet air humidity ratio, while it decreases with the increase of wheel speed, regeneration air temperature, and regeneration mass flowrate.

3. The area of the solar air collector A_c increases with the increase of inlet air humidity ratio, wheel speed, and regeneration air temperature, while, it decreases with the increase of inlet air temperature, regeneration mass flowrate and solar radiation.

4. The efficiency of the solar air collector η_c increases with the increase of inlet air temperature, and inlet air humidity ratio, wheel speed, regeneration air temperature, while decrease with the increase of regeneration mass flowrate, heat exchanger effectiveness and ground source circulation effectiveness.

5. The cooling coil load $Q_{c.c}$ increases with increase of inlet air temperature, and inlet air humidity ratio, wheel speed, and regeneration air temperature while decrease with the increase of regeneration mass flowrate, heat exchanger effectiveness and ground source circulation effectiveness.

6. The coefficient of performance increases COP_{th} with increase heat exchanger effectiveness and ground source circulation effectiveness, while decrease with the increase of inlet air temperature, and inlet air humidity ratio, wheel speed and regeneration air temperature.

7. the hybrid system is more efficient than the vapor compression system.

NOMENCLATURE

The following symbols are used in this paper:

- A_c = area of solar collector, m^2 ;
 COP_{th} = coefficient of performance;
 C_p = specific heat, $J/kg\ K$;
 I = solar radiation, W/m^2 ;
 h_i = enthalpy, J/kg ;
 \dot{h}_1 = thermal losses to the glass cover by natural convection, $w/m^2\ K$;
 \dot{h}_{r21} = thermal losses to the glass cover by thermal radiation, $w/m^2\ K$;
 \dot{h}_{r23} = thermal losses to the glass cover by the bottom plate by thermal radiation, $w/m^2\ K$;
 \dot{h}_4 = convection heat transfer coefficient of fluid on the bottom plate, $w/m^2\ K$;
 \dot{h}_w = convection heat transfer coefficient from the glass covers due to wind, $w/m^2\ K$;
 \dot{h}_{rs} = radiation heat transfer coefficient from the glass cover to sky, $w/m^2\ K$;
 U_b = conduction heat transfer coefficient across the insulation, $w/m^2\ K$;
 \dot{h}_3 = convection heat transfer coefficients for the fluid, $w/m^2\ K$;
 m = mass flow rate, kg/s ;

m^*f = Air mass flow rate per unit area of collector

N = wheel speed, RPH;

q_u = Energy gain, W/m^2 ;

T = temperature;

T_1 = ambient temperature, k ;

T_s = sky temperature, $^{\circ}K$;

T_C = Mean temperature on the glass cover, k ;

T_{ap} = Mean temperature on the absorbing plate k ;

T_f = mean air temperature, k ;

T_{bp} = mean temperature on the bottom plate, k ;

T_a = ambient air temperature,

T_{fi} = inlet temperature to solar collector, k ;

T_{fo} = outlet temperature from solar collector, k ;

τ_c = Transmissivity of solar radiation of the glass cover;

U = velocity of air, m/s ;

V_w = wind velocity of the ambient air (m/s);

α_{ap} = absorptivity of solar radiation of the absorbing plate;

η_c = efficiency of solar collector; and

ω_i = humidity ratio.

REFERENCES

- [1] S. P. Halliday, C. B. Beggs, P. A. Sleigh, "The use of solar desiccant cooling in the UK: a feasibility study". Applied Thermal Engineering, 1327-1338, 2002.
- [2] H. M. Henninga, T. Erpenbeck, C. Hindenburg, "The potential of solar energy use in desiccant cooling cycles". International journal of Refrigeration, 220-229, 2001.
- [3] J. C. Sheridan, J. W. M. Witchell, "A hybrid solar desiccant cooling system", Solar energy, vol 34(7), 187-193, 1985.
- [4] P. R. Burns, J. W. Mitchell, W. A. Beckman, "Hybrid desiccant cooling systems in super market applications, ASHRAE Trans 91 (Part-1B), 457-468, 1985.
- [5] M. Singh, S. Jain, S. C. Kaushik, "Energy conservation through hybrid air conditioning cycles: computer modeling studies", Applied Thermal Engineering, 580-591, 1995.
- [6] GA. Florides, SA. Tassou, SA. Kalogirou, LC. Wrobel "Review of solar and low energy cooling technologies for buildings". Renewable and Sustainable Energy Reviews, vol 6:557-572, 2002.
- [7] D. La, Y.J. Dai, Y. Li, R.Z. Wang, T.S. Ge, "Technical development of rotary desiccant dehumidification and air conditioning: a review". Renewable and Sustainable Energy Reviews, vol 14,130-147, 2010.
- [8] D.G. Waugaman, A. Kini, C.F. Kettleborough, "A review of desiccant cooling systems", Journal of Energy Resources Technology, vol 115, 1-8,2010.
- [9] P. Mazzei, F. Minichiello, D. Palma, "HVAC dehumidification systems for thermal comfort: a critical review", Applied Thermal Engineering vol 25, 677-707, 2004.
- [10] K. Daou, R.Z. Wang, Z.Z. Xia, "Desiccant cooling air conditioning: a review", Renewable and Sustainable Energy Reviews, vol 10, 55-77, 2006.
- [11] J.J. Jurinak, J.W. Mitchell, W.A. Beckman, "Open-cycle desiccant air conditioning as an alternative to vapor compression cooling in residential applications", Journal of Solar Energy Engineering, vol 106, 252-260,1984.
- [12] P.L. Dhar, S.K. Singh, "Studies on solid desiccant-based hybrid air-conditioning systems", Applied Thermal Engineering, vol 21, 119-134, 2001.
- [13] C.X. Jia, Y.J. Dai, J.Y. Wu, R.Z. Wang, "Analysis on a hybrid desiccant air conditioning system", Applied Thermal Engineering, vol 26 2393-2400, 2006.
- [14] S.A. El-Agouz, and A.E. Kabeel, "Performance of desiccant air conditioning system with geothermal energy under different climatic conditions". Energy Conversion and Management, vol 88, pp. 464-475, 2014.
- [15] M. Sultan, and T. Miyazaki, "Energy-Efficient Air-Conditioning Systems for Nonhuman Applications". Refrigeration, (pp.97-117), 2017.

- [16] M. Kashif, M. Sultan, and Z. M Khan, "Alternative Ai Conditioning Options for Developing Countries". *Eur. J. Eng. Res. Sci*, vol. 2, pp. 76–79, 2017.
- [17] H. Niaz, M. Sultan, A.A. Khan, T. Miyazaki, Y. Feng, and Z.M. Khan, "Study on evaporative cooling assisted desiccant air conditioning system for livestock application in Pakistan". *Fresenius Environ. Bull.*, vol. 28, pp. 8623–8633, 2019.
- [18] M.H. Mahmood, M. Sultan, and T. Miyazaki, "Solid desiccant dehumidification-based air-conditioning system for agricultural storage application: Theory and experiments". *Proc. Inst. Mech. Eng. Part A J. Power Energy*, vol. 234, pp. 534–547, 2019.
- [19] Sh. Noor, H. Ashraf, M. Sultan, and Z.M. Khan, "Evaporative cooling options for building air-conditioning: A comprehensive study for climatic conditions of Multan (Pakistan)". *Energies*, vol. 13, pp. 1-23, 2020.
- [20] M. Sultan, H. Niaz, and T. Miyazaki, "Investigation of Desiccant and Evaporative Cooling Systems for Animal Air-Conditioning". *Low Temp. Technol. Energies*, vol. 13, pp. 5530, 2020.
- [21] D. B. Jani, Manish Mishra, P. K. Sahoo, "Solid desiccant air conditioning – A state of the art review". *Renewable and Sustainable Energy Reviews*, Vol. 1451-1469, 2016.
- [22] T. Kusuda, and P.R. Archenbach, "Earth temperature and thermal diffusivity at selected stations in the United States". *ASHRAE Trans*71, vol. 1, pp. 61–74, 1965.
- [23] V. Khalajzadeh, and M. Farahani, G. Heidarinejad, "A novel integrated system of ground heat exchanger and indirect evaporative cooler". *Energy Build*, vol. 49, pp. 604–610, 2012.
- [24] J.A. Duffie, and W.A. Beckman, "Solar engineering of thermal processes". *Technical and documentation*, John Wiley & Sons: 2nd Ed (1991).